Computational Intelligence in Electrical Engineering
Vol. 12, No. 4, 2022
Research Paper

# A Compromise Solution based on Fuzzy Decision Making for multi-objective Hourly Planning in Clustered Microgrids Considering Uncertainty of Renewable Energy Resources

Reza Saki[1], Esmaeel Rokrok[*1], Meysam Doostizadeh[1], Mohammad Abedini[2]

[1] Department of Electrical Engineering, Lorestan University, Khorramabad, Iran
saki.re@fe.lu.ac.ir, rokrok.e@lu.ac.ir, doostizadeh.me@lu.ac.ir

[2] Department of Electrical Engineering, Ayatollah Borujerdi University, Borujerd, Iran
m.abedini@abru.ac.ir

**Abstract :**
This paper proposes a multi-objective function for hourly optimization of microgrids performance through minimizing the operating costs, losses and, voltage deviation index. A fuzzy decision-maker is used in this study to select the best solution from the optimally set goals by the Pareto Front beam method. In this paper, the collections of microgrids are separated into several clusters and power transaction between clusters as well as between distribution system and MG clusters, with consideration for the uncertainty of renewable energy resources (RESs), is examined. An hourly robust energy management approach is presented for distribution systems under the penetration of renewable energy-based MGs. In addition to wind turbines and photovoltaics as RESs, the MGs are equipped with energy storage systems and micro-turbines. The uncertainty of renewable generation is demonstrated via the information gap decision theory (IGDT) technique. To validate the effectiveness of the proposed model, it is tested on a 94 bus distribution test system using the general algebraic modeling system (GAMS) software. The results show the prominence of MGs clustering in improving the techno-economic characteristics of the distribution system and indicate the important consequences of clustered microgrids in optimal power transaction and distribution system operation.

**Keywords:** Video Clustered microgrids- Fuzzy decision making - Information Gap Decision Theory - Renewable energy resources.

## 1. Introduction

### 1.1. Motivation

The growing development of energy consumption has led to a global energy crisis in recent years. Therefore, energy systems have an important role in modern societies. The several profits of smart microgrids, make them an actual remedy for improving the operation of distribution systems. Microgrids (MGs) can contribute to energy transactions and deliver the anticipation of the distribution system hub. The traditional methods of electrical energy transmission have undertaken some revisions. The traditional structure of the distribution network leads to some historical problems [1]. Wall Street Journal reported, a cyber-attack on only nine electrical substations in the United States will cause main blackouts in the country [2]. By applying the energy resources in distribution systems, smart MGs are formed as an

[1] Submission date: 04, 04, 2020
Acceptance date: 08 , 09, 2020
Corresponding author: Esmaeel Rokrok, Department of Electrical Engineering - Lorestan University - Khorramabad – Iran

approach to deal with those challenges. However, applying MGs requires advanced technology for controlling and managing several experiments such as technical restrictions and coordination to distribution system parameters [3]. Clustered MGs (CMGs) are collections of MGs and a division of a distribution system. In present distribution systems, the distributed energy resources (DERs) seem vital to supply system loads under several conditions. The energy storage system (ESS) has an important role in DER to improve network performance. It can be used both as a load and as energy storage in the network [4]. Limitation of renewable energy resources (RESs) and ESSs impact on network efficiency [5]. They have a number of restrictions, such as uncertainty of RESs, feeder capacity limits, increasing feeder losses and power flow constraints. For overcoming these constraints, CMGs have been presented in this paper.

Feeder capacity constraint is considered for MGs which are connected via several independent links and lead to a reduction in energy losses via distribution feeders. Hourly robust energy management approach (REMA) is presented for distribution systems under the penetration of RESs. In addition to wind turbines (WTs) and photovoltaics (PVs) as RESs, the MGs are equipped with an energy storage system (ESS) and micro-turbines (MTs).

### 1.2. Literature Survey

By reviewing recent works on energy management in distribution systems, respected results can be seen; nevertheless, they have some drawbacks in comparison to this study. In [3] multi-vector energy management approach is proposed for islanded microgrid clusters, taking into account the role of resources and loads in optimally managing the energy flow through the CMGs. In [2], a bi-level optimization problem is presented in for energy management of a distribution system consisting of a community of MGs, with the economical, operational, and environmental objectives. In [4], the communication between MGs and distribution network is considered as the main aspect for improving the effective performances of the distribution systems. Reference [5] motivated on improving the faults in the energy planning of CMGs by a real-time distribution compensation method, which is used to the local MGs. Predictive control model based on energy management framework, is presented in [6]. In this reference authors have tried to minimize the interaction between the distribution system and community of MGs. The suggested algorithm was responsible for optimal organization of different energy resources with the network of MGs, taking into consideration diverse operational, economical, and environmental limitations. A chance-constrained control strategy is proposed in [7] for improving the local operation of networked microgrids in the presence of renewable-based distributed generations and storage devices. In [8], a transactive control strategy is introduced for managing the charging/discharging energy pattern of energy storage systems to decline the peak load condition caused by electric vehicles (EVs). Reference [9] has concentrated on voltage control issues of CMGs considering the medium and low voltage levels individually. The work existing in [10] has taken into consideration the frequency regulation of networked MGs by regulating a frequency reference point for MGs locally; then it applied the tertiary control approach to manage the flow of power through the point of common of each MG. A three-level multi-layer control strategy is introduced in [11] which coordinated the operation strategies of energy storage devices and sub-MGs. In [12], a three-step analysis is performed to investigate the role of MGs as resilience resources in boosting the resilience of the distribution system, where a new MG formation is introduced to explore the resilience of multi-energy MGs. Finally, the distribution network reconfiguration is adopted in [13] to connect islanded MGs to decline load curtailment as much as possible. In terms of stability, different voltage and current stabilizer controllers are used in [14] to regulate voltage and current of CMGs, where the proposed control algorithm is defined as a plug-and-play controller. In [15] the chance of communicating different points of MGs, that are equipped with a drop controller, to form a larger grid is examined. Reference [16] applied the small-signal analysis for the management and control of large grids. In [17], the MGs are

connected via distribution system arrangements to form CMGs that are strong in face of uncertainty of renewable-based generation units, improvement the entire system resilience, and reservation it from instability which can result in shutdowns. Table 1 presents the taxonomy of existing literature on scheduling and improving the operation of the distribution system.

**Table (1): Taxonomy of existing literature on planning and improving the operation of the distribution system**

| Reference | RES | FDM | DRP | MOF | Clustering | Optimization Method | | IGDT |
|---|---|---|---|---|---|---|---|---|
| | | | | | | GAMS | Heuristic | - |
| [6] | ✓ | - | - | - | - | - | - | - |
| [7] | ✓ | - | - | ✓ | - | - | ✓ | - |
| [8] | ✓ | - | - | - | - | - | ✓ | - |
| [9] | ✓ | - | - | ✓ | ✓ | - | ✓ | - |
| [10] | ✓ | - | - | - | ✓ | - | ✓ | - |
| [11] | ✓ | - | - | - | ✓ | - | ✓ | - |
| [12] | ✓ | - | - | ✓ | - | - | ✓ | - |
| [13] | ✓ | - | - | ✓ | - | - | - | - |
| [14] | ✓ | - | ✓ | - | ✓ | ✓ | - | - |
| [15] | ✓ | - | ✓ | - | ✓ | - | - | - |
| [16] | ✓ | - | ✓ | - | - | - | ✓ | - |
| [17] | ✓ | - | - | - | - | - | ✓ | - |
| [18] | ✓ | - | - | - | - | - | ✓ | - |
| [19] | ✓ | - | - | ✓ | - | - | ✓ | - |
| This study | ✓ | ✓ | ✓ | ✓ | ✓ | ✓ | - | ✓ |

### 1.3. Contributions

This paper presents CMGs with RESs technologies, the demand response program (DRP) and ESSs. Optimal power transactions among CMGs and the grid are determined. Therefore, this article has the following innovations:

- Robust energy management strategy (REMA) with hourly state of switches, improves system security, alleviates feeders' congestion, and increases reliability.
- The role of ESS and DRP of MGs in REMS is highlighted
- By applying a fuzzy decision-maker method to select a compromise solution in complex multi-objective problems, economical and technical indexes have improved.

### 1.4. Paper organization

The structure of this paper is organized as follows. Section 2 discusses the modeling of the proposed method. Section 3 gives the mathematical formulation of the proposed method and the solution method. Section 4 presents the test case and its clustering structure. Section 5 shows and discusses the numerical results and Section 6 draws the conclusions.

## 2. Modeling and formulation

### 2.1. Objective Functions

The objective functions in this problem are defined in the form of three objective functions including the cost function of the generation units in each MG, the voltage deviation index (VDI), and the cost of active power losses as described in Eqs (1) -(3).

$$GC^{Total} = \sum_{t\in\Omega_t}\sum_{i\in\Omega_b} P_{i,t}^{Net}\times\lambda_t + \sum_{t\in\Omega_t}\sum_{i\in\Omega_{MG}} P_{i,t}^{CMG}\times\lambda_t \quad (1)$$

$$VDI = \sum_{t\in\Omega_t}\sqrt{\sum_{i\in\Omega_b}\frac{(V_{j,t}-1)^2}{\Omega_b}} \quad (2)$$

$$P_{loss} = \sum_{t\in\Omega_t} P_t^{loss} \quad (3)$$

The active power that flows between MGs should be limited in distribution systems. Power balance must be met in each MG, while MGs can import or export energy from /to other MGs or distribution systems.

AC load flow is mentioned in Eqs (4)-(9).

$$P_{i,t}^{Net} + \sum_{m\in\Omega_{MG}} P_{m,t}^{MG} - P_{i,t}^{D} = V_{i,t}\sum_{j\in\Omega_b}\wp_{ij,t}^{L}\times V_{j,t}\times(G_{ij}\cos\theta_{ij,t} + B_{ij}\sin\theta_{ij,t}) \quad (4)$$

$$Q_{i,\mathrm{t}}^{Net} + \sum_{m\in\Omega_{MG}} Q_{m,\mathrm{t}}^{MG} - Q_{\mathrm{i,t}}^{D} = V_{i,\mathrm{t}} \sum_{j\in\Omega_b} \wp_{ij,t}^{L} \times V_{\mathrm{j,t}} \times (G_{ij}\sin\theta_{ij,\mathrm{t}} - B_{ij}\cos\theta_{ij,\mathrm{t}}) \quad (5)$$

$$V_i^{\min} \le V_{i,t} \le V_i^{\max} \quad (6)$$

$$\left(I_{R_{ijt}}^2 + I_{M_{ijt}}^2\right) \le I_{MAX_{ij}}^2 \quad (7)$$

$$I_{R_{ijt}} = \wp_{ij,t}^{L} \times \left\{ \begin{matrix} G_{ij}\left(V_{i,\mathrm{t}}\cos\theta_{i,\mathrm{t}} - V_{j,\mathrm{t}}\cos\theta_{j,\mathrm{t}}\right) \\ -B_{ij}\left(V_{j,\mathrm{t}}\sin\theta_{i,\mathrm{t}} - V_{j,\mathrm{t}}\sin\theta_{j,\mathrm{t}}\right) \end{matrix} \right\} \quad (8)$$

$$I_{M_{ijt}} = \wp_{ij,t}^{L} \times \left\{ \begin{matrix} G_{ij}\left(V_{i,\mathrm{t}}\sin\theta_{i,\mathrm{t}} - V_{j,\mathrm{t}}\sin\theta_{j,\mathrm{t}}\right) + \\ B_{ij}\left(V_{j,\mathrm{t}}\cos\theta_{i,\mathrm{t}} - V_{j,\mathrm{t}}\cos\theta_{j,\mathrm{t}}\right) \end{matrix} \right\} \quad (9)$$

MGs limitations containing load flow constraints and DRP, and restraining loads in certain hours have been deliberated in the REMA. So, the amount of active and reactive power is limited by the systems agent. In addition, limitations are imposed on the ESSs, where the most important limitations on their charging and discharging status are the corruption of these resources. RESs limitations are other constraints that are straightly related to the energy consumption of microgrids. The modeling and equations for each constraint of the MGs are discussed.

The limitations on active and reactive power balances in each MGs must be considered in the hourly programming. These constraints are shown in the equations which include the balancing of the active and reactive generation power in the MGs. The active and reactive power imported/exported among CMGs and of other clusters must be equal to the sum of the power generated by their DERs. In Eqs (10) and (11) these subjects are seen.

$$P_{m,\mathrm{t}}^{MG} = P_{m,t}^{WT} + P_{m,t}^{PV} + P_{m,t}^{MT} + \left(P_{m,t}^{DisCh} - P_{m,t}^{Ch}\right) - P_{m,t}^{DR} \quad (10)$$

$$Q_{m,t}^{MG} = Q_{m,t}^{WT} + Q_{m,t}^{MT} - Q_{m,t}^{DR} \quad (11)$$

The DRP constraints are clear as restraining the amount of active and reactive power loads to a definite value. According to (14) and (15), the variations forms in the demand will be equal to the sum of base loads after applying the DRP. The DRP program is demonstrated in Eqs (12) - (16).

$$P_{m,t}^{DR} = P_{m,t}^{L} \times \Lambda_{m,t}^{DR} \quad (12)$$

$$Q_{m,t}^{DR} = Q_{m,t}^{L} \times \Lambda_{m,t}^{DR} \quad (13)$$

$$\sum_{t\in\Omega_t} P_{m,t}^{DR} = \sum_{t\in\Omega_t} P_{m,t}^{L} \quad (14)$$

$$\sum_{t\in\Omega_t} Q_{m,t}^{DR} = \sum_{t\in\Omega_t} Q_{m,t}^{L} \quad (15)$$

$$(1-\Lambda_m^{Min}) \le \Lambda_{\mathrm{m},t}^{DR} \le (1-\Lambda_m^{Max}) \quad (16)$$

ESSs constraints contain charging and discharging can be done by applying the charging and discharging factor at the charging and discharging power (17), (18). The charge state parameter limitation is also shown in Eqs (20), (21).

$$0 \le P_{\mathrm{m},t}^{Ch} \le \kappa_{\mathrm{m},t}^{ch} \times P_{\mathrm{m},t}^{ch_{\max}} \quad (17)$$

$$0 \le P_{\mathrm{m},t}^{DisCh} \le \kappa_{\mathrm{m},t}^{dch} \times P_{\mathrm{m},t}^{dch_{\max}} \quad (18)$$

$$\kappa_{\mathrm{m},t}^{Ch} + \kappa_{\mathrm{m},t}^{DisCh} \le 1\ ,\ \ (\kappa_{\mathrm{m},t}^{Ch}, \kappa_{\mathrm{m},t}^{DisCh} \in \{0,1\}) \quad (19)$$

$$SOC_{\mathrm{m},t}^{ESS} = SOC_{\mathrm{m},t}^{ESS} + \Delta t.(P_{\mathrm{m,t}}^{Ch}\ \mu_{\mathrm{m,t}}^{ch} - P_{\mathrm{m,t}}^{DisCh} / \mu_{\mathrm{m,t}}^{dch}) \quad (20)$$

$$SOC_m^{\min} \le SOC_{\mathrm{m},t}^{ESS} \le SOC_m^{\max} \quad (21)$$

$$\sum_{t\in\Omega_t} P_{\mathrm{m},t}^{Ch} \ge \sum_{t\in\Omega_t} P_{\mathrm{m},t}^{DisCh} \quad (22)$$

Limitation of MTs reactive power is presented by its generation between zero and maximum under normal operating conditions. Eqs. (23), and (24) illustrate these restrictions.

$$0 \le P_{m,t}^{MT} \le P_{m,t}^{MT_{\max}} \quad (23)$$

$$Q_{m,t}^{MT_{\min}} \le Q_{m,t}^{MT} \le Q_{m,t}^{MT_{\max}} \quad (24)$$

The predicted power of the WTs is determined by the prediction coefficient. Hence, the active power generated is restricted by this coefficient and it is restricted by the lag or lead angle of reactive power. Limitation of WTs is demonstrated in Eqs (25), (26).

$$0 \le P_{m,t}^{WT} \le P_{m,t}^{WT_{\max}} \times \alpha_t^{WT} \quad (25)$$

$$-tg(\varphi_{lead}) \times P_{m,t}^{WT} \le Q_{m,t}^{WT} \le tg(\varphi_{lag}) \times P_{m,t}^{WT} \quad (26)$$

The predicted power of the PVs is determined by the prediction coefficient which is shown in Eq (27).

$$0 \le P_{m,t}^{PV} \le P_{m,t}^{PV_{\max}} \times \rho_t^{PV} \quad (27)$$

## 2.2. Branches Constraints

Branches constraints contain the state of the switches between MGs and clusters. The state of switches is presented by a decision variable that it's designed in the optimization problem.

$$\Gamma_{mn,t}^{MG} = 1 \quad , \forall i \in \Omega_C \; and \; j \in \Omega_C \tag{28}$$

$$\Gamma_{mn,t}^{MG} \in \{0,1\} \quad , \forall m \notin \Omega_C \; or \; n \notin \Omega_{MG} \tag{29}$$

## 2.3. Multi-Objective

There are several methods to multi-objective optimization, the most important of which are comparative as follows.

### 2.3.1 Weighted sum

In this method, each objective is allocated a scalar weight that indicates its relative importance to other objectives. The optimization problem is then turned into optimizing the weighted sum of different objective functions. The multiple objective optimization problem is transformed into a single objective problem by using a weighted sum of the original multiple objectives. Although the weighted sum method is the simplest and most straightforward way of obtaining multiple points on the Pareto-optimal front, it does not work in finding the non-convex optimal cost. It is hard to select the weighting to ensure that the points are spread evenly on the Pareto front and it is difficult as well in finding all the optimal cost by changing the weights.

### 2.3.2 ε − Constraint

$\varepsilon -$ Constraint method has been commonly used as an interactive decision-making tool owing to its easy implementation. This method is also known as a trade-off method, which means that the decision-maker specifies a trade-off among the multiple objectives. In this method, one of the objectives is optimized while the others are treated as constraints. This method works in finding the non-convex optimal cost [18].

In this paper optimization problem is a non-convex problem, so the $\varepsilon -$ constraint method is the most efficient method compared to other methods. This is noteworthy that heuristics methods have a problem with the uniqueness of the answer, due to the long convergence, and they are not efficient for hourly planning.

## 2.4. Min-max Fuzzy decision-maker (FDM)

In this section, we have studied the optimization of objective functions through the $\varepsilon -$ constraint method in order to find the best compromise solution through the Pareto Front and Fuzzy Satisfying methods. In the proposed REMA problem, $VDI$ is optimized while $P_{loss}$ and $GC^{Total}$ are considered as the constraints as in Eqs (30)-(32).

$$OF = \min(VDI) \tag{30}$$

s.t

$$P_{loss} \le \varepsilon_1 \tag{31}$$

$$GC^{Total} \le \varepsilon_2 \tag{32}$$

It is observed from Fig. 2 and Eqs (30)-(32) that $P_{loss}$ and $GC^{Total}$ are constrained by parameter $\varepsilon$. This parameter varies from the minimum value to the maximum value of $P_{loss}$ and $GC^{Total}$ gradually, and for any value of $P_{loss}$ and $GC^{Total}$, the modified single objective optimization problem, i.e., (1-29), is solved, and the optimal solutions like in Fig. 1 are obtained. It is noteworthy to mention that in (30) the constraints of the original multi-objective optimization problem, i.e., (1) - (29), which are described in Section 2, are also included. The set of all obtained solutions for the entire variations of $\varepsilon$ is Pareto front of the multi-objective optimization problem.

By solving the REMA problem, a Pareto front is derived and it is required to select the best solution from this Pareto optimal set. The fuzzy decision-maker is used in this paper for this purpose. In this method, a fuzzy membership function is apportioned to each solution in the Pareto front. The fuzzy sets are defined by membership functions. These functions show the degree of membership in fuzzy sets using values from 0 to 1[19]. The membership value '0' indicates inconsistency with the sets, while '1' means compatibility. Fuzzy membership functions that assign a degree of approval to each objective are defined based on which the best solution can be found out of the available Pareto-optimal solutions.

The best compromise solution which can be selected is designated by using the min-max method. In the min-max method the minimum value of $f_1$ , $f_2$ and $f_3$ for each solution is

determined, and the solution with the maximum value of $\min(f_1, f_2, f_3)$ is selected as the best compromise solution. The membership functions are calculated as follow:

$$\Phi_\rho(f_i)=\begin{cases}1 & f_i \le f_i^{\min}\\ \dfrac{f_i^{\max}-f_i}{f_i^{\max}-f_i^{\min}} & f_i^{\min} \le f_i \le f_i^{\max}\\ 0 & f_i \le f_i^{\max}\end{cases}, \forall \rho \in \mu, i \in \Delta$$

where $\rho$ refers to the $\rho$th solution of the $i$th objective function. $\mu$ in this study has 10 members. $f_i$ is the membership objective function for the fuzzy decision, with the maximum value of $f_i$ calculated for the minimum value of $f_{i'}$ (i.e., $i' = \Delta - \rho$). This means that the maximum value of $f_i$ is obtained when $f_{i'}$ is optimally minimized. $f_i$ is also assigned to the smallest value of the membership objective function $f_i$. The best solution can then be selected using the fuzzy min-max proposition as follow:

$$\Theta = \max_{\rho \in \mu}\left\{\min_{i \in \Delta}\left\{\Phi_\rho(f_i)\right\}\right\}$$

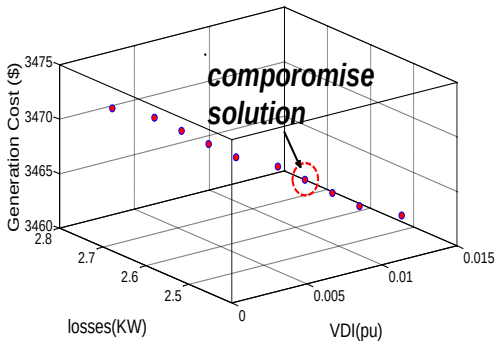


**Fig. 1. Description of Pareto front in $\varepsilon$ -constraint method.**

The best compromise solution which can be selected is described in [20] by using the min-max method. In the min-max method the minimum value of $\Phi_1$ , $\Phi_2$ and $\Phi_3$ for each solution is determined, and the solution with the maximum value of min ( $\Phi_1$ , $\Phi_2$ , $\Phi_3$ ) is selected as the best compromise solution. In this paper, $\Phi_1$ , $\Phi_2$ and $\Phi_3$ are calculated as (33)-(35).

$$\Phi_1 = \frac{VDI^{\max} - VDI_k}{VDI^{\max} - VDI^{\min}} \quad (33)$$

$$\Phi_2 = \frac{GC^{Total\,\max} - GC_k^{Total}}{GC^{Total\,\max} - GC^{Total\,\min}} \quad (34)$$

$$\Phi_3 = \frac{P_{loss}^{\max} - P_{loss,k}}{P_{loss}^{\max} - P_{loss}^{\min}} \quad (35)$$

By solving the MO-HEM problem, a Pareto front is derived and it is required to select the best solution from this Pareto optimal set. The fuzzy decision-maker is used in this paper for this purpose. In this method, a fuzzy membership function is assigned to each solution in the Pareto front. The fuzzy membership is in the interval (0,1).

Table 4 shows the values for the objective function before CMGs and REMA and after CMGs and REMA in 24 hours. It is clear that by applying REMA in the presence of CMG, objective function of losses (OF loss), VDI and Generation cost (G cost) are decreased. This point is important that the numerical value of every objective function has been achieved based on every 24 hours.

**Table 4 Values for objective functions**

| | Before REMA | After REMA |
|---|---|---|
| Loss(MW) | 2.849 | 2.578 |
| VDI (pu) | 0.015 | 0.007 |
| G Cost($) | 3473.56 | 3464.771 |

## 3. IGDT Approach

Information gap decision theory (IGDT) is a famous decision-making tool which was introduced by Ben-Haim in 2006 [21]. IGDT has superiority over other techniques such as scenario-based, and Monte Carlo approaches that have been demonstrated in [22]. Also, the accuracy of the results obtained from IGDT over other methodologies has been examined in [23]. Lastly, the general merits of the IGDT technique are highlighted in [24] and compared with available uncertainty modeling techniques. Commonly, the IGDT technique is formulated as follows:

$$f = \min_x \left\{ f(X, \iota) \right\} \quad (1)$$

$$I_i(X, \iota) \le 0 \quad , \forall i \in \Omega_{ineq} \quad (2)$$

$$Z_j(X, \psi) = 0 \quad , \forall j \in \Omega_{eq} \quad (3)$$

$$\iota \in \upsilon\left(\tilde{\iota}, \alpha\right) \quad (4)$$

where $\iota$ is the uncertain input parameter, while $x$ is the set of decision variables; the behavior of uncertain parameter is described by $\upsilon$. The uncertainty set can be mathematically described as:

$$\forall \iota \in \upsilon\left(\bar{\iota},\alpha\right)=\{\iota:|\frac{\iota-\bar{\iota}}{\bar{\iota}}|\le\alpha\} \quad (5)$$

In (5), $\bar{\iota}$ is the predicted value of the uncertain parameter, while $\alpha$ denotes the radius of uncertainty. Generally, the IGDT technique is a bi-level optimization problem that is solved in two levels. The first level, called the base case (BC) is solved without consideration for uncertainty, and there is no deviation between the uncertain parameter and its forecasted value. To describe this level, the following equations are used.

$$of_b=\min_x\left\{f\left(X,\bar{\iota}\right)\right\} \quad (6)$$

$$I_i\left(X,\bar{\iota}\right)\le 0 \quad ,\forall i\in\Omega_{ineq} \quad (7)$$

$$Z_j\left(X,\bar{\iota}\right)=0 \quad ,\forall j\in\Omega_{eq} \quad (8)$$

$$\max_x \alpha \quad (9)$$

$$I_i\left(X,\bar{\iota}\right)\le 0 \quad ,\forall i\in\Omega_{ineq} \quad (10)$$

$$Z_j\left(X,\bar{\iota}\right)=0 \quad ,\forall j\in\Omega_{eq} \quad (11)$$

$$f\left(X,\iota\right)\le of_b\left(X,\bar{\iota}\right)\times\left(1+\beta\right) \quad ,\iota\in\upsilon \quad (12)$$

$$0\le\beta\le 1 \quad (13)$$

$$\alpha\ge 0 \quad (14)$$

The amount of objective function in (6) is obtained in a deterministic optimization problem and considered as the BC for the next level. The second level can be solved from two viewpoints namely, (a) RAS: this strategy is chosen by risk-averse decision-maker which tries to increase the robustness of the system in face of uncertainty, and (b) opportunity seeker strategy: this strategy is followed by optimistic decision-maker which accepts the level of chance to decrease the value of the objective function from its predicted value in the BC. Since this study aims at maximizing the robustness of the whole distribution network including CMGs, it uses the RAS. Accordingly, the objective function, in this case, will be increased by a tolerable value which is defined by decision-maker, while it tries to maximize the uncertainty radius. Consequently, the result obtained from this strategy has a degree of robustness, even if the uncertain parameter would fluctuate.

## 4. Test Study and Simulation Parameters

The test study and simulation parameters are presented in this section. The effects of CMGs on the distribution system are also studied. The IEEE 94-bus distribution test system [27], as shown in Fig. 2, is used for simulation purposes. It consists of 37 branches, 32 sectionalizing switches, and 5 tie switches. The proposed complete framework of this study can be easily adapted to any other large-scale network. Construction is implemented on the standard 94 bus distribution test system in Portuguese. It is supposed that 10 MGs are connected to this network, and the MGs are clustered in three groups according to table 2. The location of each MG and the structure of networked MGs, as well as the interconnection paths, are shown on the one-line diagram of the test system in Fig. 2. The data of this system is available in [27]. The proposed problem is simulated as a mixed-integer non-linear programming (MINLP) in GAMS [27] environment using SBB solver. The distribution system load demand pattern, electricity price, and predicted output power of PVs and WTs are given in Table 3. The rated power of WTs, PVs, and MTs that have been installed in each MG, and the load of MGs are given in [9].

**Table (2): MGs clustered**

| | |
|---|---|
| Cluster 1 | MG1-MG5 |
| Cluster 2 | MG7-MG8-MG10 |
| Cluster 3 | MG2-MG3-MG4-MG6-MG9 |

The proposed model is solved for a 24 hours' performance perspective.

**Table (3): Forecasted hourly demand, output power of WTs & PVs, energy price.**

| Time (hour) | Ritio of Demand to peack load(%)[27] | $\alpha_t^{WT}$ wind | $\rho_t^{PV}$ PV | Energy price($/MW) [27] |
|---|---|---|---|---|

| | | | | |
|---|---|---|---|---|
| 1 | 0.719 | 0.815 | 0 | 28 |
| 2 | 0.674 | 0.880 | 0 | 24 |
| 3 | 0.624 | 0.886 | 0 | 22 |
| 4 | 0.588 | 0.880 | 0 | 22 |
| 5 | 0.582 | 0.881 | 0 | 23 |
| 6 | 0.588 | 0.881 | 0 | 25 |
| 7 | 0.600 | 0.953 | 0 | 27.5 |
| 8 | 0.633 | 0.987 | 0.008 | 31.5 |
| 9 | 0.644 | 0.985 | 0.050 | 37.5 |
| 10 | 0.730 | 0.962 | 0.125 | 44 |
| 11 | 0.793 | 1.000 | 0.418 | 42.5 |
| 12 | 0.844 | 0.979 | 0.511 | 40 |
| 13 | 0.875 | 0.945 | 0.516 | 42 |
| 14 | 0.868 | 0.776 | 0.475 | 43 |
| 15 | 0.851 | 0.673 | 0.418 | 46 |
| 16 | 0.875 | 0.591 | 0.254 | 47.5 |
| 17 | 0.951 | 0.487 | 0.050 | 48.5 |
| 18 | 1.000 | 0.466 | 0 | 48.5 |
| 19 | 0.981 | 0.373 | 0 | 50 |
| 20 | 0.948 | 0.339 | 0 | 44.5 |
| 21 | 0.900 | 0.339 | 0 | 38 |
| 22 | 0.875 | 0.372 | 0 | 36 |
| 23 | 0.801 | 0.393 | 0 | 30 |
| 24 | 0.722 | 0.339 | 0 | 26 |

## 5. Numerical Results

In this section, the results obtained for the proposed REMA are discussed. Then the effects of clustering on the distribution system are also examined. The hourly output power from PV, WT, and MT in each MG is demonstrated in Figs. (3), (4) and (5). These figures show the hourly planning power output for each DG in CMGs; this planning is done by the distributing system agent based on REMA. Output power from PV before 7 and after 17 is zero. It is noteworthy to mention that according to unequal constraints for power generation of DGs (Eqs 23 - 27) if power generation by DGs is more than power generation that the agent has decided for that DG in a special time, that extra power is curtailed to the upstream network, or otherwise it is saved by ESSs or charging stations of EVs. Curtailment power is the difference between the maximum of DG generation power and the maximum power that the agent defines for DGs based on the optimal condition. According to Figs. (3), (4) and (5) for example, it is illustrated that applying REMS, OF loss in 24 hours is 2.85 MW. Thereby in 24 hours distribution system and MGs losses, 280 KW is reduced.

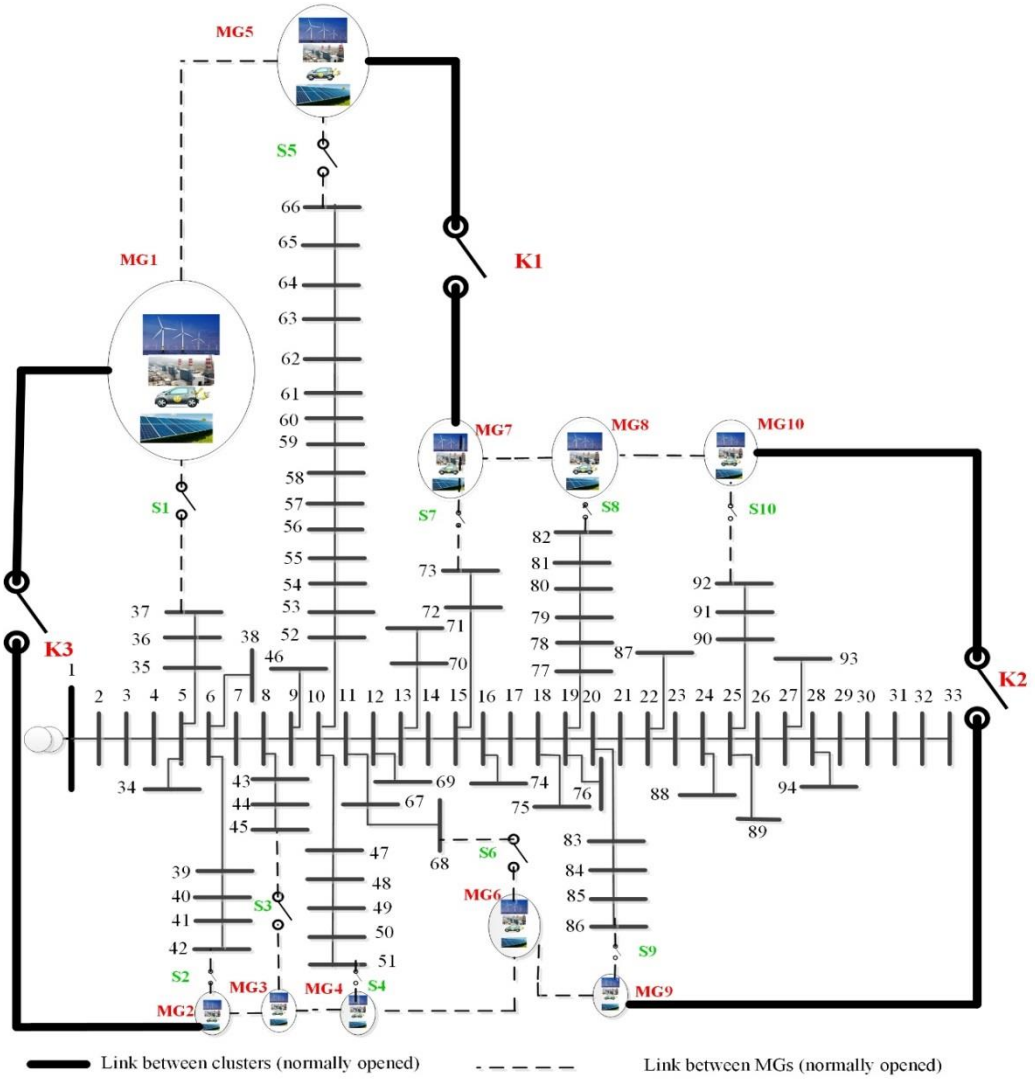


**Fig. 2. Single line diagram of 94 bus actual Portuguese distribution test system.**

The SOC of ESS in each cluster is shown in Figs. 7, 8, and 9. Cluster number 3 has the maximum SOC and this phenomenon is illustrated by applying HEMS. ESSs are active sources in MGs. For example, in clusters at the time between 2 to 7, ESSs are charged, and at the time between 17 to 22, they are discharged. Fig. 6 shows the power transaction among clusters and the distribution system. For example, cluster#1, in half of the 24 hours, delivers energy to the distribution system in optimal conditions.

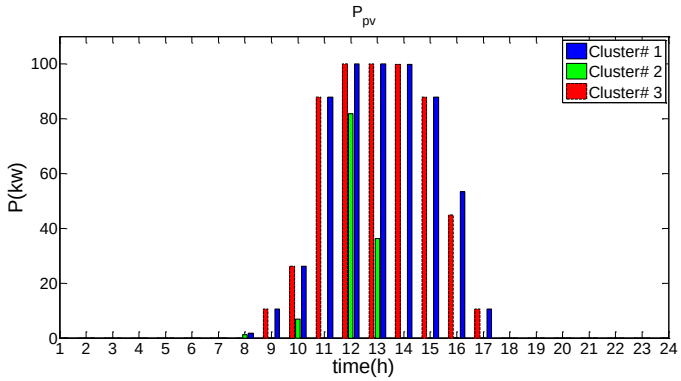


**Fig.3.Hourly output power from PV in MGs**

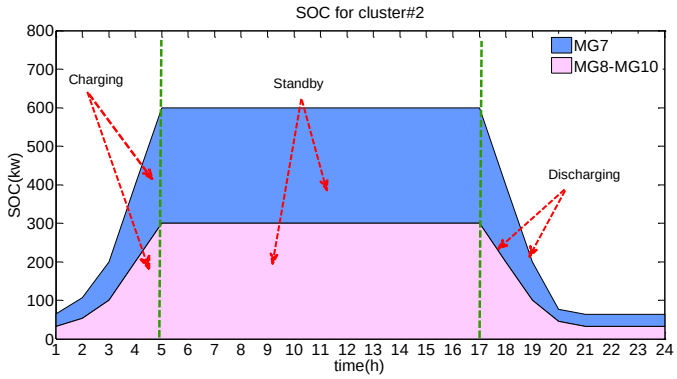


**Fig.4.Hourly output power from MT in MGs**

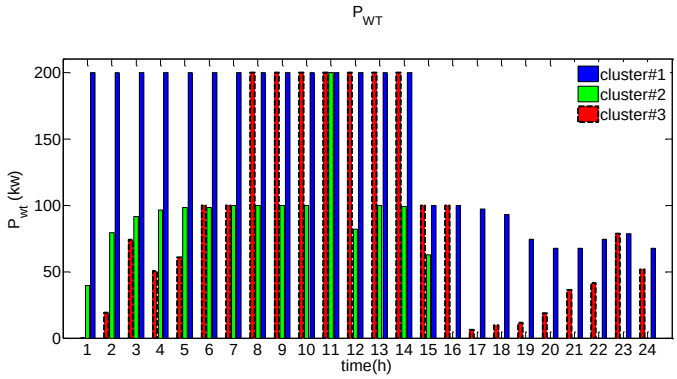


**Fig. 5.Hourly output power from WT in MGs**

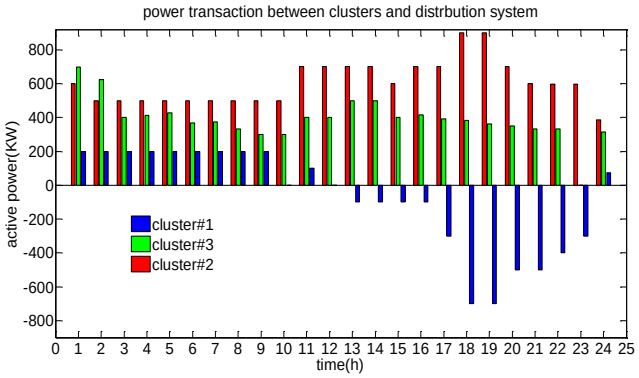


**Fig. 6. Hourly power transaction among clusters and the distribution system**

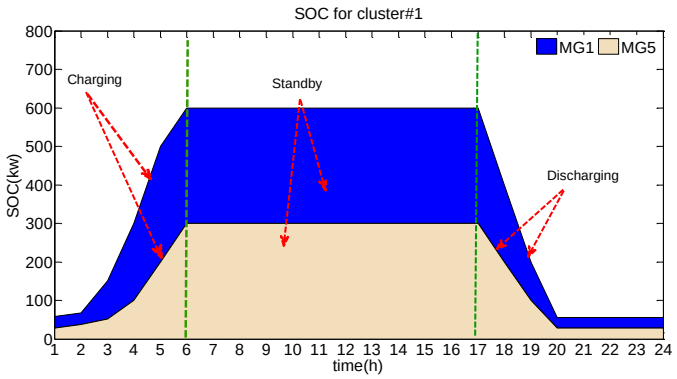


**Fig. 7. Hourly SOC of ESS in cluster 1**

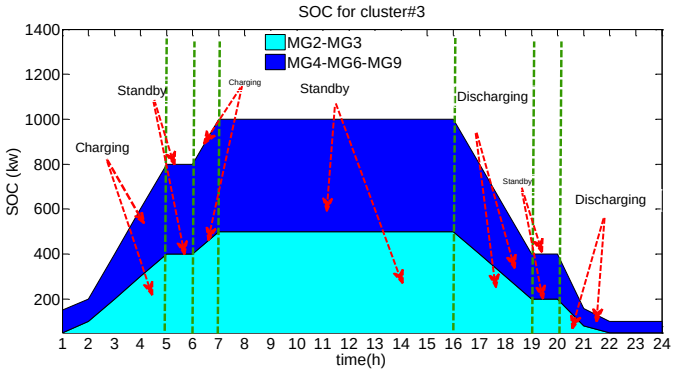


**Fig. 8. Hourly SOC of ESS in cluster 2**

Hourly voltage constraint condition in buses that have heavy loads compared with and without applying REMA is shown in Figs. 10, 11. It is clear that after applying this framework, the voltage profile is improved. In other words, in this paper, technical constraints are considered and they are improved after this plane. The active power losses of distribution network in this two condition is illustrated in Fig. 11. According to this figure, power losses of the system with REMA is 1,038 KW lower than that of without these technologies, which demonstrates the importance of CMGs in declining the power losses. The status of switches per hour among clusters and between MGs to the network is illustrated in table 5. It is clear that many loads that are settled in MGs, in many hours, are provided by the clusters. Therefore, switches that connect clusters are often closed.

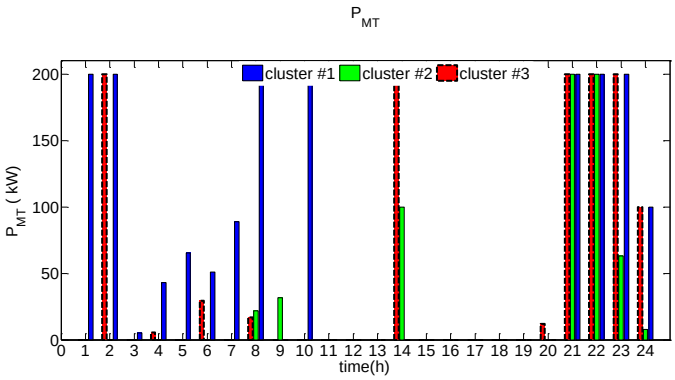


**Fig. 9. Hourly SOC of ESS in cluster 3**

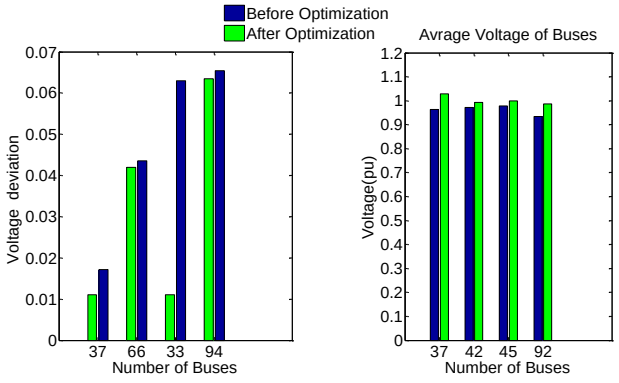


**Fig.10. Hourly voltage profile before optimization**

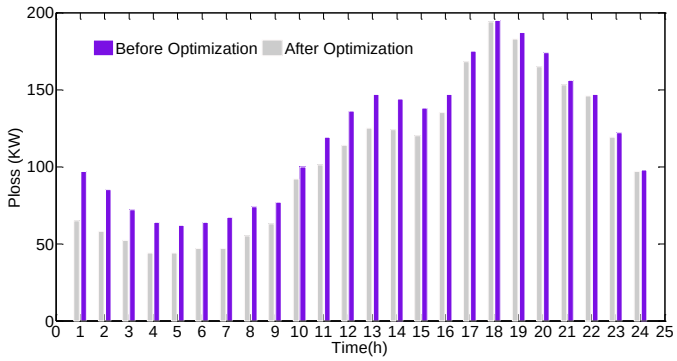


**Fig .11. Active power loses of the distribution system in two scenarios**

The variation of the DRP index in MGs of different clusters is shown in Fig. 7. It is evident from this figure that the behavior of responsive loads is different in each cluster. Besides, it can be seen that the customers increased their consumption rate in off-peak hours, while they consumed lower load in on-peak hours; which means the DSO can benefit from the DRP of CMGs.

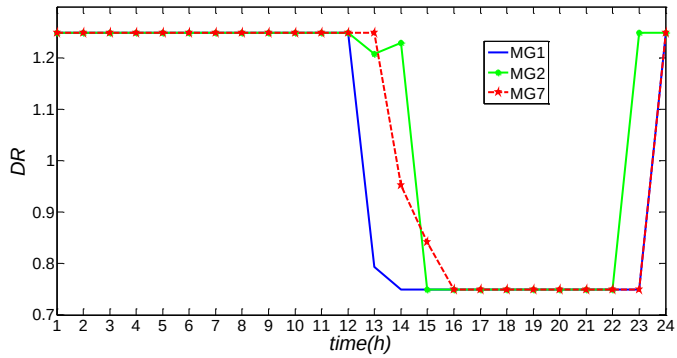


**Fig .12. Variation of DR index in different clusters**

**Table (5): The status of switches per hour among clusters and between MGs to network**

| Time (hour) | S1 | S2 | S3 | S4 | S5 | S6 | S7 | S8 | S9 | S10 | K1 | K2 | K3 |
|---|---|---|---|---|---|---|---|---|---|---|---|---|---|
| 1 | Off | Off | Off | On | On | On | On | On | On | On | On | Off | On |
| 2 | Off | Off | Off | On | On | On | On | On | On | On | On | Off | On |
| 3 | Off | Off | Off | Off | On | On | On | On | On | On | On | Off | On |
| 4 | Off | Off | Off | On | On | On | On | On | On | On | On | Off | On |
| 5 | Off | Off | Off | On | On | On | On | On | On | On | On | On | On |
| 6 | Off | Off | Off | Off | On | Off | On | On | On | On | On | On | On |
| 7 | Off | Off | Off | Off | On | Off | On | On | On | On | On | On | On |
| 8 | Off | Off | Off | Off | On | Off | On | On | On | On | On | On | On |
| 9 | Off | Off | Off | Off | On | Off | On | On | On | On | On | On | On |
| 10 | On | Off | Off | Off | On | Off | Off | On | On | On | On | On | On |
| 11 | On | Off | Off | Off | On | Off | On | On | On | On | On | On | On |
| 12 | On | Off | Off | Off | On | Off | On | On | On | On | On | On | On |
| 13 | On | Off | Off | Off | On | Off | On | On | On | On | On | On | On |
| 14 | On | Off | Off | Off | On | Off | On | On | On | On | On | On | On |
| 15 | On | Off | Off | Off | On | Off | On | On | On | On | On | On | On |
| 16 | On | Off | Off | Off | On | Off | On | On | On | On | On | On | On |
| 17 | On | Off | Off | Off | On | Off | On | On | On | On | On | On | On |
| 18 | On | Off | Off | Off | On | Off | On | On | On | On | On | On | Off |
| 19 | On | Off | Off | Off | On | Off | On | On | On | On | On | On | On |
| 20 | On | Off | Off | Off | On | Off | On | On | On | On | On | On | On |
| 21 | On | Off | Off | Off | On | Off | On | On | On | On | On | On | Off |
| 22 | On | Off | Off | Off | On | Off | Off | On | On | On | On | On | Off |
| 23 | On | Off | Off | Off | On | Off | Off | On | On | On | On | Off | On |
| 24 | Off | Off | Off | Off | Off | Off | Off | On | On | On | On | Off | On |

## 6. Conclusion

In this paper, the REMA strategy is proposed for MGs in clusters. To improve the techno-economic characteristics of the distribution system, each MG is equipped with ESSs, WTs, MTs, PVs, and responsive loads, while the MGs and clusters connected via switch links. The proposed model aims at minimizing the operation cost, losses and, VDI of the distribution system, which can receive energy from upstream networks and MG clusters. The simulation result shows that the distribution system can benefit from CMGs and MGs. In summary, the main conclusions are as follows:

1. The IGDT method leads to the optimal design of switching statues in the REMA framework.

2. The distribution system should inject more active power to the CMGs to increase the strength of the entire system, including the network of CMGs, against uncertainty.

3. Case studies demonstrated that up to 40% of MGs total loads is provided by ESSs in some hours. Hence, ESS charging/discharging pattern plays a key role in REMA.

4. Both DRP and CMGs improve distribution system characteristics and prevent load shedding during daily operation of the distribution system.

5. Having applied REMA decreases total systems power losses and indicate the importance of CMGs in declining the power losses.

## Appendix

### Nomenclature

**Indices**

| | |
|---|---|
| $i, j$ | Index for distribution system buses |
| $l$ | Index for distribution system transmission lines |
| $t$ | Index for time |
| $m, n$ | Index for the network of MGs |

**Sets**

| | |
|---|---|
| $\Omega_b$ | Set of system distribution system buses |
| $\Omega_l$ | Set of distribution lines |
| $\Omega_b^{MG}$ | Set of distribution system buses which are connected to MG |
| $\Omega_{MT}$ | Set of MT |
| $\Omega_{PV}$ | Set of PV |
| $\Omega_{ESS}$ | Set of ESS |
| $\Omega_{WT}$ | Set of WT |
| $\Omega_C$ | Set of clusters |
| $\Omega_t$ | Set of time |

**Parameters**

| | |
|---|---|
| $P_{i,t}^D / Q_{i,t}^D$ | Active/reactive power consumption of load connected to bus i at time t |
| $P_{m,t}^L / Q_{m,t}^L$ | Active /reactive power consumption of MG nodes |
| $\Lambda_m^{Max} / \Lambda_m^{Min}$ | Maximum flexibility of responsive loads |
| $P_{m,t}^{MT_{max}}$ | Maximum active power of MT |
| $P_{m,t}^{WT_{max}}$ | Maximum active power of WT |
| $P_{m,t}^{PV_{max}}$ | Maximum active power of PV |
| $\mu_{m,t}^{ch/dch}$ | Charging/discharging efficiencies of ESSs |
| $G_{ij} / B_{ij}$ | Conductance/ susceptance of line between buses i and j (pu) |
| $\Gamma_{mn,t}^{MG}$ | Binary variable stating the connectivity status of clusters (1 = connected, 0 = not connected) |
| $V_i^{max/min}$ | Maximum/minimum voltage magnitude |
| $I_{M_{ijt}}$ | Imaginary current flow of distribution lines |
| $P_{m,t}^{PV_{max}}$ | Maximum active power of PV |
| $SOC_{m,t}^{ESS}$ | State of charge of ESS installed in bus m at time t (pu) |
| $\Delta t$ | Timeslot Duration (hr) |

**Variables**

| | |
|---|---|
| $P_{i,t}^{Net} / Q_{i,t}^{Net}$ | Active/reactive power injected from substation to bus i at time t |
| $P_{ij,t} / Q_{ij,t}$ | Active/reactive power flow that leaves bus i toward node j |
| $P_{i,t}^{CMG}$ | Active power injected/entered from/to MG to/from distribution system |
| $P_{m,t}^{MG} / Q_{m,t}^{MG}$ | Active/reactive power transfer between MGs |
| $P_{mt}^{WT} / Q_{mt}^{WT}$ | Active/reactive power output of WT |
| $P_{mt}^{PV}$ | Active power output of PV |
| $P_{mt}^{MT} / Q_{mt}^{MT}$ | Active/reactive power output of MT |
| $P_{m,t}^{DisCh}$ | Active power discharge of ESS |

| | |
|---|---|
| $P_{m,t}^{Ch}$ | Active power charge of ESS |
| $P_t^{loss}$ | Hourly active power losses |
| $P_{m,t}^{DR} / Q_{m,t}^{DR}$ | Active/reactive power consumption of MG nodes after applying the DR program |
| $\Lambda_{m,t}^{DR}$ | Demand response index |
| $\alpha_t^{WT}$ | Forecasted available wind power |
| $\rho_t^{PV}$ | Forecasted available solar power |
| $\kappa_{m,t}^{ch} / \kappa_{m,t}^{dch}$ | Charging/discharging decisions of ESSs (1 = allowed, 0 = not allowed) |
| $P_{m,t}^{Ch} / P_{m,t}^{DisCh}$ | Charge/discharge power of ESS installed at bus m at time t (pu) |
| $P_{m,t}^{ch_{max}} / P_{m,t}^{dch_{max}}$ | Maximum charging/discharging rate of ESS at an hour (KW) |
| $\wp_{ij,t}^{L}$ | Binary variable stating the connectivity status of MGs |
| $I_{R_{ijt}}$ | Real current flow of distribution lines |
| $I_{M_{ijt}}$ | Imaginary current flow of distribution lines |
| $I_{MAX_{ij}}$ | Maximum current flow between buses i and j |
| $SOC_m^{max/min}$ | Maximum/minimum SOC of ESS installed at bus m |
| $\theta_{ij,t}$ | Phase angle between buses i and j at time t |
| $\theta_{i,t} / \theta_{j,t}$ | Phase angle for buses i / j at time t |
| $\varphi_{lead/lag}$ | Lag or lead angle of reactive power |
| $V_{i,t} / V_{j,t}$ | Voltage magnitude of bus i /j at time t |
| $\lambda_t$ | Electric energy price ($/MWh) |

## References


[1] Saleh. M, Althaibani. A, Esa. Y, A. Mohamed, "Impact of clustering MGs on their stability and resilience during blackouts," International Conference on Smart Grid and Clean Energy Technologies (ICSGCE) pp.195 – 200, 2015

[2] Tweed. K, "Attack on Nine Substations Could Take Down U.S. Grid," IEEE Spectrum, 2014.

[3] Shuaia. Z, YingyunSun. B, JohnShen. Z, et al, "MG stability:Classification and a review," Renewable and Sustainable Energy Reviews, Vol.58, pp.167–179, 2016

[4] Anurag. C, Saini. R, "A review on Integrated Renewable Energy System based power generation for stand-alone applications Configurations,storage options,sizing methodologies and control," Renewable and Sustainable Energy Reviews, Vol.38, pp.99–120, 2014.

[5] Kianmehr. E, Nikkhah. S, Vahidinasab.V, et al, "A Resilience-based Architecture for Joint Distributed Energy Resources Allocation and Hourly Network Reconfiguration," IEEE Transactions on Industrial Informatics, Vol. 15, pp.1-12, 2019.

[6] Yang. M, W. Yanwei, Yang. F, et al," Hierarchical control for DC microgrid clusters with high penetration of distributed energy resources," Electric Power Systems Research , Vol.148 , pp.14-20, 2017.

[7] Xiong. X, wang. J, Jing. T, et al,"Power optimization control of microgrid cluster," Electric Power Automation Equipment," Vol. 37, pp. 10-17, 2009

[8] Mehta. R , Srinivasan. D , Trivedi. A , et al,"Hybrid Planning Method Based on Cost-Benefit Analysis for Smart Charging of Plug-In Electric Vehicles in Distribution Systems," IEEE Transactions on Smart Grid, Vol. 10 , pp. 523 – 534, 2019.

[9] Lu. T, Zhaoyu. W , Qian. A , Lee. W," Interactive Model for Energy Management of Clustered Microgrids," IEEE Transactions on Industry Applications , Vol. 53 , pp. 1739 – 1750, 2017.

[10] Palizban. O, Kauhaniemi. K,"Energy storage systems in modern grids—Matrix of technologies and applications," Journal of Energy Storage, vol. 6, pp. 248-259, 2016.

[11] Osama. R. A, Zobaa. A. F and Abdelaziz. A, "A Planning Framework for Optimal Partitioning of Distribution Networks Into Microgrids," in IEEE Systems Journal, Vol. 14, No. 1, pp. 916-926, 2020.

[12] Khavari. F, Badri. A, Zangeneh. A and Shafiekhani. M ,"Energy management in multi-microgrids via an aggregator to override point of common coupling congestion," IET Generation, Transmission & Distribution, Vol. 13 , pp. 634 - 642 , 2019.

[13] Asimakopoulou. G. E, Dimeas. A. L and Hatziargyriou. N. D, "Leader-Follower Strategies for Energy Management of Multi-Microgrids," IEEE Transactions on Smart Grid, Vol. 4, pp. 1909-1916, 2013.

[14] Nunna. H and Doolla. S, "Demand Response in Smart Distribution System With Multiple Microgrids," IEEE Transactions on Smart Grid, Vol. 3, pp. 1641-1649, 2012.

[15] Nick. M, Cherkaoui. R and Paolone. M, "Optimal Planning of Distributed Energy Storage Systems in Active Distribution Networks Embedding Grid Reconfiguration," IEEE Transactions on Power Systems, Vol. 33, pp. 1577-1590, 2018.

[16] Arasteh. H, Sepasian. M. S, and Vahidinasab. V, "An aggregated model for coordinated planning and reconfiguration of electric distribution networks," Energy, Vol. 94, pp. 786–798, 2016.

[17] Wang. Y, Mao. S and Nelms. R, "On Hierarchical Power Scheduling for the Macrogrid and Cooperative Microgrids," IEEE Transactions

on Industrial Informatics, Vol. 11, pp. 1574-1584, 2015.

[18] Liu. X, Gao. B, Zhu. Z, et al, "Non-cooperative and cooperative optimization of battery energy storage system for energy management in multi-microgrid, "IET Gener. Trans. Distrib, Vol 25, pp. 2369–2377, 2018.

[19] Wang. X, Gong. Y and Jiang. C, "Regional Carbon Emission Management Based on Probabilistic Power Flow With Correlated Stochastic Variables," IEEE Transactions on Power Systems, Vol. 30, pp. 1094-1103, 2015.

[20] Jafari. A, Shahbazian. A, Fereidunian. A , Nikoofard. A, "Improving self-healing of smart distribution network by allocating switches and distributed generation resources using soft computing," Computational Intelligence in Electrical Engineering, Vol. 11, , 2020.

[21] Chiandussi. C, Codegone. M, Ferrero. M , "Comparison of multi-objective optimization methodologies for engineering applications," Computers & Mathematics with applications, Vol. 63, pp.912-942, 2012.

[22] Nasr. M, Nikkhah. S, Gevork. B, et al, " A multi-objective voltage stability constrained energy management system for isolated microgrids," Electrical Power and Energy Systems, Vol. 117, 2020.

[23] Soroudi. A, Rabiee. A, Keane. S, " Information gap decision theory approach to deal with wind power uncertainty in unit commitment," Electr Power System Research, Vol. 145, pp.137-148, 2017.

[24] Rabiee. A, Soroudi. A, Mohammadi-ivatloo. B and et al, "Corrective voltage control scheme considering demand response and stochastic wind power," IEEE Transaction on Power System, Vol.29, pp.2965-2973, 2014.

[25] Wang. X, Gong. Y, Jiang. C," Regional carbon emission management based on probabilistic power flow with correlated stochastic variables," IEEE Transaction on Power System, Vol.30, pp. 1094-1103, 2014.

[26] Soroudi. A, Siano. P, Keane. A, "Optimal DR and ESS scheduling for distribution losses payments minimization under electricity price uncertainty," IEEE Transaction on Smart Grid, Vol.7, pp. 261-272, 2016.

[27] Parvania. M,Fotuhi-Firuzabad. M, Shahidehpour. M, "Optimal demand response aggregation in wholesale electricity markets, "IEEE Transaction on Smart Grid, Vol.4, pp.1957-1965, 2013.